MATURATION OF HYDROXYAPATITE FROM BIOGENIC CALCIUM SOURCE – A COMPARATIVE STUDY

Cristina Rodica DUMITRESCU[1], Ionela Andreea NEACSU[1,2,7*], Vasile Adrian SURDU[1,2], Adrian Ionut NICOARA[1,2], Cosmin Iulian CODREA[1,3], Cristian-Emilian POP[4,5], Roxana TRUSCA[2], Ecaterina ANDRONESCU[1,2,6,7]

This research aims to synthesize hydroxyapatite powders from a biogenic calcium source (hen eggshell) and study the effect of two maturation methods (a classical method and a combined short time maturation at 135°C in microwave-assisted hydrothermal conditions) on its final properties. The synthesized specimens consist of nanometric polycrystalline particles of carbonated apatite, with enhanced osteogenic effect due to the presence of trace elements, and high crystallinity (up to 72.44%). It was concluded that the maturation conditions impacted the morpho-structural and compositional characteristics of the obtained powders, as well as their cytotoxic behavior in contact with mouse osteoblasts MC3T3-E1 culture.

Keywords: hydroxyapatite nano-powder, microwave-assisted hydrothermal maturation, eggshell, co-precipitation

1. Introduction

Alveolar bone loss defects are caused mainly by tooth extraction, severe periodontitis, or tumor surgery, and can be treated nowadays by using bone substitutes [1-4]. For alveolar ridge preservation, sinus augmentation, and periodontal bone defect reconstruction, were recently developed synthetic grafts in the form of dense or porous scaffolds, powders, injectable biomaterials, mineralized membranes, cement paste, etc. [1, 5]. For medical applications it is essential to use biomimetic substituents, therefore great attention was given to natural hydroxyapatite (HA), usually derived from animal bones and scales [6], seashells, eggshells. Their usage as Ca precursors constitutes a simple and cheap

[1] University POLITEHNICA of Bucharest, Romania; e-mails: cristinadumitrescu0@gmail.com; neacsu.a.ionela@gmail.com (*corresponding author); adrian.surdu@upb.ro; adrian.nicoara@upb.ro; cosmin.codrea@stud.chimie.upb.ro; ecaterina.andronescu@upb.ro
[2] National Research Center for Micro and Nanomaterials, University POLITEHNICA of Bucharest, Romania; truscaroxana@yahoo.com
[3] Institute of Physical Chemistry "Ilie Murgulescu" of the Romanian Academy, Romania; e-mail: ccodrea@icf.ro
[4] University of Bucharest, Romania; e-mails: pop.cristian-emilian@s.bio.unibuc.ro
[5] Non-Governmental Research Organization Biologic, Romania; contact@ngobiologic.com
[6] National Research Center for Food Safety, University Politehnica of Bucharest, Romania
[7] Academy of Romanian Scientists, 3 Ilfov str, Bucharest, Romania

method to obtain non-stoichiometric HA with important trace elements (Na, Mg, Zn, Fe, etc.) content, particularly important in osteogenic processes [7]. The inorganic mineral phase of human bone consists of poorly crystalline, calcium-deficient hydroxyapatite (HA), with HPO_4^{2-}, CO_3^{2-}, Mg^{2+}, Na^+, F^- or other ions as lattice substituents for Ca^{2+}, PO_4^{3-} or OH^- ions [8]. Literature studies showed that HA synthesized at lower temperatures exhibited a higher inflammatory response in cells and increased fibroblastic proliferation [9, 10]. Even though different synthesis approaches are available, microwave and hydrothermal methods are found to be highly advantageous because both processes are rapid and lead to the production of uniform mesoporous hydroxyapatite nanoparticles, with consistent physicochemical properties [11]. Combining these two methods proved efficient in the large-scale production of mesoporous HA nanoparticles, in a less time-consuming manner [12].

This paper proposes the synthesis of hydroxyapatite powders, with structure and composition similar to biological apatite, as prospective bone replacements. The novelty of this study derives from the synergistic effect given by the natural biogenic calcium carbonate source (eggshell) and the hybrid maturation method used, which consists of a microwave-assisted hydrothermal process (HTMW). Compared to the classic maturation of HA, at room temperature, this innovative method is expected to generate comparable morpho-structural and biological properties, but in a shorter time.

2. Materials and methods

2.1. Synthesis and maturation of hydroxyapatite

Hen eggshells from local poultry have been used as a natural calcium source. The eggshells were washed, boiled for 4 h in distilled water and H_2O_2 for complete removal of the organic part, then dried at 60°C for 24 h, and automatically ground for 15 minutes. The ground powder was calcined in an electric oven (Nabertherm) for 3h at 800°C (heating rate of 10°C/min), then slowly cooled at room temperature. The obtained powder was ground, then subjected to homogenization in 200 mL of distilled water for half an hour, until the suspension became stable. A solution of $(NH_4)_2H(PO_4)$ 38.5 wt.% was added dropwise over the obtained precipitate (2 mL/min), until a ratio of Ca/P=1.67 was obtained, periodically checking, and adjusting the pH >10. The resulting mixture was split into four samples: two samples were maintained at room temperature and atmospheric pressure for 12h (coded HA_CP_12), respectively 48h (coded HA_CP_48), corresponding to the classical maturation method; the other two samples were first exposed for 10 min to HTMW conditions, at a maximum temperature of 135°C and pressure of 16.8 bars, then slowly cooled to 25°C, before the above described classical maturation (HA_HT_12, HA_HT_48). All

aged samples were centrifuged and washed with distilled water until pH=7, then dried at 60°C for 48h.

2.2. Morpho-structural evaluation

X-Ray Diffraction (XRD) analysis was performed using a PANalytical Empyrean Diffractometer, operating in Bragg-Brentano configuration with Cu-Kα (λ= 1.5406 Å), recorded between 10°<2θ <80° with a scan speed of 0.5°/min and a step of 0.02°. The crystallinity, cell unit parameters, volume, and average crystallite size of the obtained powders were assessed using the XRD patterns, as previously described [13].

Fourier Transform Infra-Red (FTIR) spectra were recorded in the range of 4000-500 cm^{-1}, increments of 1.928 cm^{-1}, using a Nicolet iS50R spectrometer, in the attenuated total reflection mode (ATR), at room temperature, at a resolution of 4 cm^{-1}. Quantitative calculation of the substitution degree of PO_4^{3-} with CO_3^{2-} was done using equation 1, considering the absorbance values of the characteristic bands from 1415 cm^{-1} and 1020 cm^{-1} [14, 15]:

$$\frac{C}{P} = A_{1415}/A_{1020} \quad (1)$$

A Quanta Inspect F50 scanning electron microscope (SEM), equipped with field electron emission gun (FEG) and an EDS (Energy Dispersive Spectroscopy) detector, acceleration voltage of 30 kV, and point-to-point resolution of 1.2 nm was used for the morphological evaluation of the powders.

The elemental content, at ppm level, of the powders and raw eggshell material have been determined by X-Ray Fluorescence (XRF) using Thermo Scientific ARL PERFORM'X Sequential spectrometer, which works under pressure, in a He atmosphere (Thermo Scientific UniQuant soft, non-standard method).

2.3. Biological evaluation

Mouse osteoblasts MC3T3-E1 culture was grown in complete Dulbecco's modified Eagle's medium (DEM) containing 10% fetal bovine serum (Gibco, USA) at 37ºC in a humidified atmosphere with 5% CO_2. The cells were seeded at a cell density of 105 cells/cm^2 and left to adhere for 24 h. Then, the osteoblasts were incubated for the next 24 hours with different concentrations of HA powders (10, 50, 100, and 200 µg/mL) previously sterilized by exposure to ultraviolet light for one hour. Untreated cells were used as the control for all *in vitro* experiments.

The cellular viability was measured using the 3-(4,5-dimethylthiazol-2-yl)-2,5-diphenyltetrazolium bromide (MTT assay; Sigma-Aldrich, USA) assay. After 24 hours of incubation, the culture medium was removed, and the cells (MC3T3-E1) were incubated with 1 mg/mL MTT for 2 hours at 37°C. The purple formazan crystals formed in the viable cells were dissolved with 2-propanol (Sigma-

Aldrich, USA) and the absorbance was measured at 595 nm using a microplate reader (Flex Station, Molecular Devices).

The concentration of nitric oxide (NO Griess assay) in the collected culture medium after the 24 h of incubation was performed with the Griess reagent, a stoichiometric solution (v/v) of 0.1% naphthyl-ethylene-diamine dihydrochloride, and 1% sulphanilamide in 5% H_3PO_4. Increased levels of NO are related to cytotoxic effects, as this molecule relates to inflammation and apoptosis. The absorbance of mix formed by equal volumes of medium supernatants and Griess reagent was read at 550 nm using the FlexStation 3 microplate reader and the NO concentration was calculated from the $NaNO_2$ standard curve.

3. Results and discussions

The XRD analysis of the eggshell used as calcium precursor show calcite ($CaCO_3$) with hexagonal symmetry (PDF 00-005-0586) as the main mineral phase before thermal treatment, respectively lime (CaO) with cubic symmetry (PDF 00-004-0777) after calcination (Fig. 1). CaO is a very reactive compound and most likely it partially hydrates due to environmental humidity, causing the crystallization of $Ca(OH)_2$ (portlandite) with hexagonal crystal symmetry (PDF 00-044-1481).

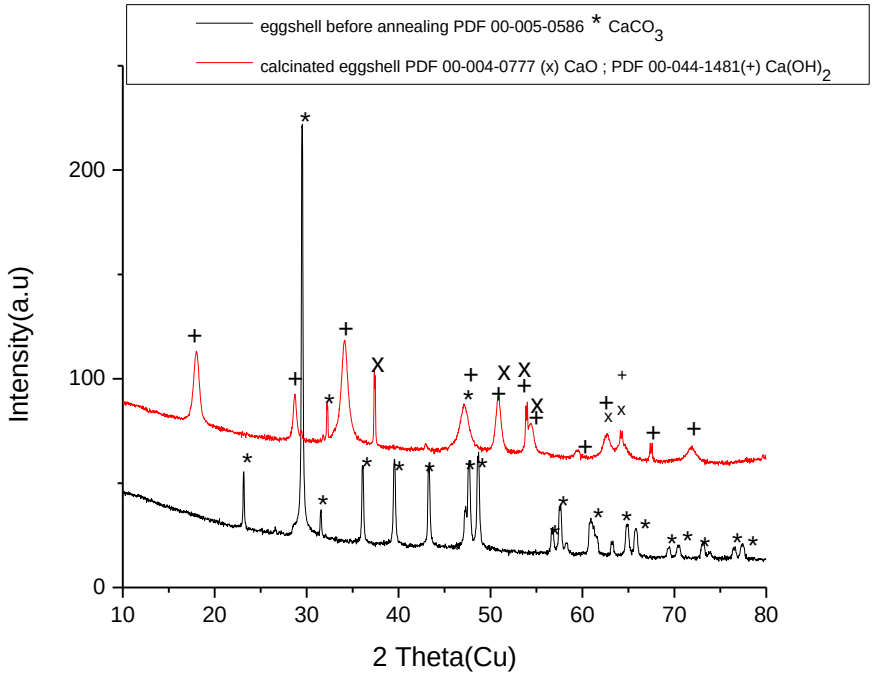

Fig. 1. X-ray diffraction plot for eggshell before annealing (black) and calcined at 800°C (red)

Ca and trace elements (Na, Mg, Mn, K, Sr, Si, Fe, Mo, Cu) contents in the eggshell before calcination and onto synthesized HA powders were determined by XRF analysis (Table 1). The presence of such minerals in synthetic hydroxyapatite was previously reported as beneficial, enhancing its osteogenic properties after grafting [16-18]. The XRF results indicate that the oligo-elements contained by the eggshell were preserved during synthesis and partially substituted the calcium ions in the hydroxyapatite lattice, giving better functional characteristics to all samples [19]. Particularly, the higher content of trace elements in the samples' outgoing classical maturation (HA_CP_12, HA_CP_48) could relate to the higher amorphous phase content in these two powders, which could better capture the metals [9, 10]. The Ca/P ratio for these samples (2.019 and 2.015 respectively) was higher than for HA-HT-12, HA-HT-48 (1.67 and 1.7 respectively) due to a superior content of amorphous calcium phosphates, whose Ca/P rates is reported between 1.5 - 2.2 in references [9, 10]. In the present case, the obtained values could be also attributed to the presence of foreign anions and cations in the HA crystal lattice. Nevertheless, it is known that the apatite from osseous tissue deviates from the theoretical stoichiometry (where Ca/P=1.67), therefore the results are promising [20-21].

Table 1

Elemental composition from XRF analysis on hen eggshell and aged HA

Sample analyzed / Identified element	Uncalcined eggshell % wt	HA_CP_12 specimen % wt.	HA_CP_48 specimen % wt.	HA_HT_12 specimen % wt.	HA_HT_48 specimen % wt.
Ca	96.38	65.6025	65.5682	60.3505	61.5527
Na	1.82	1.0345	0.9911	0.8949	0.8401
Mg	0.980	0.6542	0.6817	0.6155	0.7567
P_x	0.334	32.4869	32.5300	36.0982	36.1201
S_x	0.233	0.0762	0.0912	0.0823	0.0688
K	0.0669	0.0091	0.0106	0.0096	0.0019
Sr	0.0626	0.0325	0.0330	0.0298	0.0485
Si	0.0720	0.0681	0.0619	0.0559	0.0650
Cl	0.0163	0.0112	0.0106	0.0114	0.0101
Fe	0.0141	0.0067	0.0084	0.0135	0.0117
Mo	0.0105	0.0042	0.0039	0.0661	0.0066
Zn	0.030	0.0015	0.0045	0.0038	0.0032
Ca/P	-	2.019	2.015	1.671	1.70

X-ray diffraction analysis of all aged powders (Fig. 2) shows the representative diffraction peaks of hydroxyapatite with hexagonal (H) or monoclinic (M) symmetry, according to the PDF4+ reference sheets [01-080-7126] and [04-016-1185]. Each phase content (wt. %) is specified in Table 2. It can be observed that the powders subjected to HTMW have a higher crystallinity degree (from the Rietveld refinement method), compared to the ones aged in the classical route. No other secondary calcium phosphate phases were observed,

which suggests that a 12-48 h maturation period, even in normal conditions, is sufficient to obtain a stable hydroxyapatite phase.

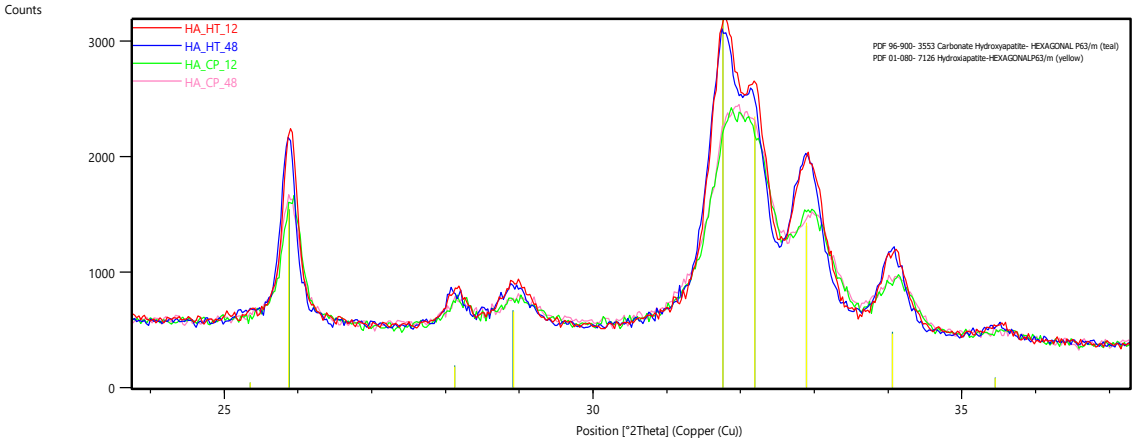

Fig. 2. X-ray diffraction profiles of the main intense peaks for all specimens

Table 2

Unit cell parameters calculated by Rietveld refinement method

Sample	HA_CP_12		HA_CP_48		HA_HT_12		HA_HT_48	
Unit Cell characteristics / Phase symmetry	M 23.5%	H 76.4%)	M 17.7%	H 82.31%	M 94%	H 6%	M 97%	H 3%
a (Å)	9.617	9.417	9.671	9.4084	9.4562	9.6313	9.4326	9.3049
b (Å)	19.231	9.417	19.257	9.4084	18.8647	9.6313	18.8522	9.3049
c (Å)	6.881	6.884	6.883	6.8856	6.8853	6.8559	6.8840	6.8802
V (Å^3)	1084.7	528.7	1048.8	527.8	1060.2	550.7	1057.8	515.8
α (°)	90	90	90	90	90	90	90	90
β (°)	90	90	90	90	90	90	90	90
ϒ (°)	120.5	120	121.0	120	120.31	120	120.2	120
Average crystallite size (nm)	33.8642		35.6023		37.9256		38.6276	
Standard deviation (nm)	193.6687		195.2428		195.3257		195.9872	
Micro-strains (%)	0.37935		0.6766		0.63205		0.5142	
Crystallinity (%)	33.95		36.61		60.46		72.44	

Moreover, the additional 10 minutes of HTMW treatment induced a tendency to crystalize in monoclinic symmetry (M) and an increase in the average crystallite size of HA_HT_12 and HA_HT_48 (more than double compared to HA_CP_12 and HA_CP_48). For the two samples aged under normal conditions, most crystals have hexagonal symmetry, as reported in the literature for synthetic HA [12]. The results are supported by literature studies which state that microwave irradiation, coupled with high pressure from the hydrothermal

treatment, generates instantaneous heating in the volume of the reaction mixture, favoring only the nucleation rate and not the one of the crystal growth [17]. Rietveld refinement revealed small deviations in the unit cell parameters of all obtained HA, attributed to the substitutions with the previously identified trace elements. Compositional and structural studies on human or mammalian bone have highlighted the duality of these phases (M and H) in which HA is present in bone tissue [8, 14].

The FTIR absorption spectra for all samples, grouped by the maturation method, are presented in Fig. 3. They are extremely similar and confirm that all powders are constituted of HA crystals, due to the identified bending and stretching vibrations of PO_4^{3-} and HPO_4^{2-} groups characteristic to hydroxyapatite [8]. FTIR spectra also highlighted the absence of absorption peak for stretching vibration of H-O bond in (OH^-), so-called "structural water", usually placed after 3500 cm^{-1}. The absorbed water was observed between 3200-3500 cm^{-1} for all samples [22, 23].

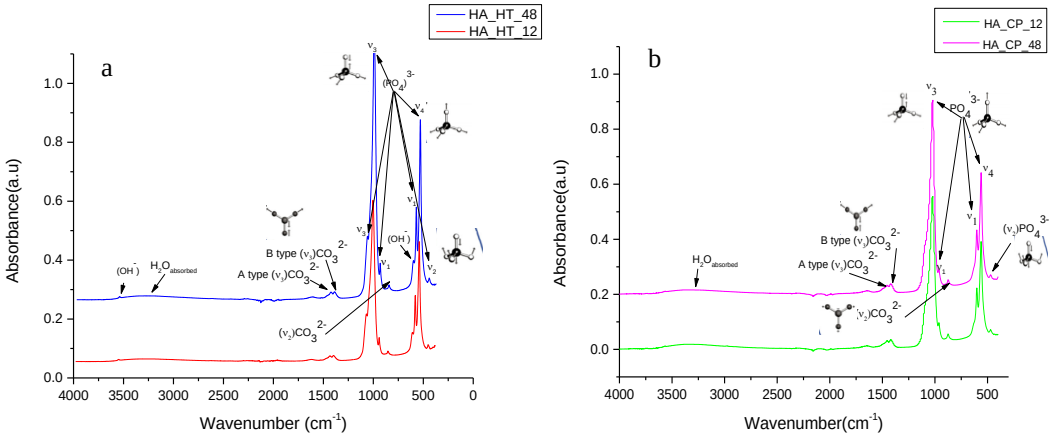

Fig. 3. FTIR spectra for (a) HA_HT_12, HA_HT_48, (b) HA_CP_12, HA_CP_48

Carbonated hydroxyapatite is known to exhibit various types of vibrations characteristic to CO_3^{2-} functional groups, having a trigonal planar symmetry D3h; active IR ν_2 (out of plane bending) appears at 871 cm^{-1}, ν_3 at 1454, 1420 cm^{-1} and ν_4 around 669 cm^{-1} in some cases poorly marked [15]. Vibration mode ν_1 (symmetrical stretching) manifests itself especially when the structure changes to a lower one and is not found in the natural bone. The exact occupancy and location of the carbonate ions in the lattice are evasive due to the nano-dimensions of the apatite crystallites [8]. According to the literature, for the quantitative calculation of the CO_3^{2-} content in natural bone, the intensity ν_2 is taken into account, which better shows the type B substitution. Specifically, the presence of a peak towards 880 cm^{-1} indicates the presence of CO_3^{2-} groups in monovalent anionic position, position ν_3 from 1420-1450 cm^{-1} can be superimposed over

amide groups in the organic component of the bone [8]. Using equation 1, it was evaluated the content of carbonate groups involved in phosphate groups substitution, in the four powders, as the rate between the heights peaks of the wavenumber 1415 and 1020 cm^{-1}, counted using OriginLab9 software [24]. The results C/P show that the highest carbonate content is found in HA_CP_12 (C/P=0.074) and HA_CP_48 (0.063), decreases at 0.039 in HA_HT_12 and remains constant (0.040) for the second sample aged in HTMW conditions. This variation may be associated with the crystallinity of the powders and the higher amounts of carbonates captured in the amorphous phase of hydroxyapatite formed.

SEM images at 100,000x magnification reveal powders with similar fluffy textures (Fig. 4 a-e) for all samples. The particles have a high tendency to agglomerate and are difficult to distinguish in size and shape. These morphological aspects are specific to HA powders synthesized by co-precipitation and could demonstrate the nano-size of the obtained HA particles [22].

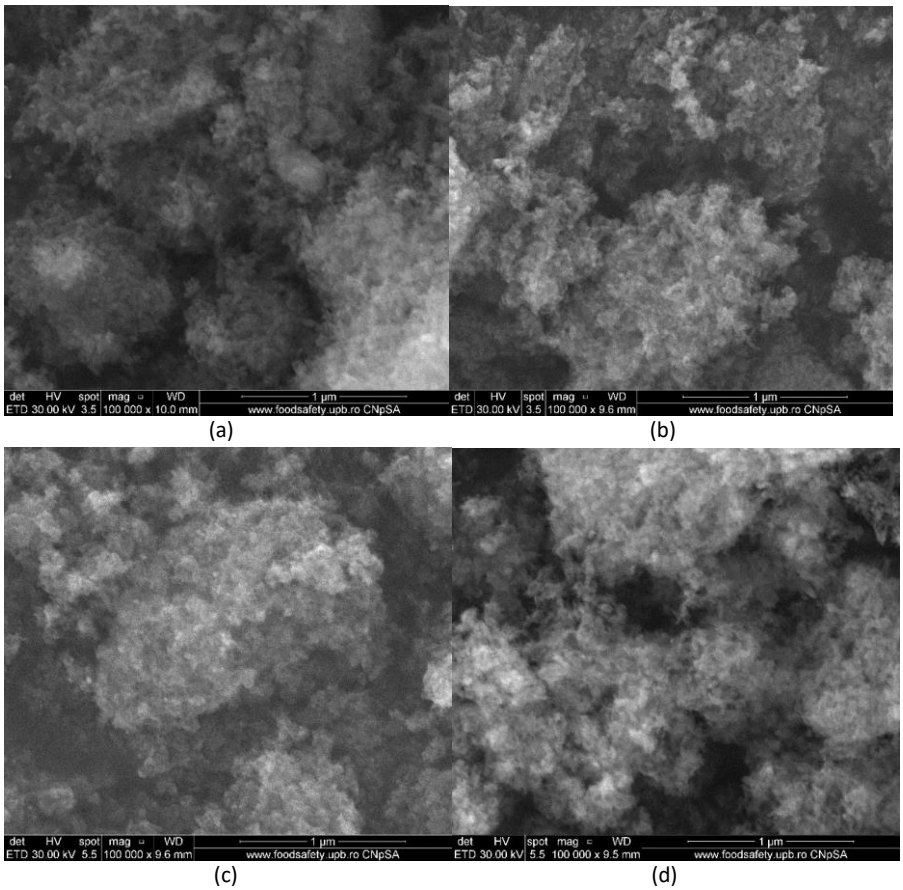

Fig. 4. SEM images for: a) HA_HT_12; b) HA_HT_48; c) HA_CP_12; d) HA_CP_48

Energy Dispersive Spectroscopy (EDS) analysis (table 3) reveals the presence of elements specific to hydroxyapatite (Ca, P, O), along with trace elements as substituents (following XRF results). However, the Ca/P ratio for the synthesized samples is not the theoretical stoichiometric one Ca/P= 1.67. This aspect is characteristic of carbonated hydroxyapatite, for which the reported Ca/P ratio varied between 1.20-2.0 [21, 25].

Table 3

Comparative EDS elemental composition for all samples

Sample	HA_HT_12	HA_HT_48	HA_CP_12	HA_CP_48
Element	Atomic %			
O K	61.02	68.08	80.23	69.11
P K	13.68	11.65	6.92	11.3
Ca K	23.62	19.4	10.8	18.67
Mg K	0.75	0.4	1.28	0.65
Na K	0.8	0.87	0.62	0.18
Si K	0.06	0.04	0.05	0.08
Ca/P	1.72	1.66	1.3	1.65

The effect of samples on cellular viability was studied by MTT assay. As shown in Fig. 5a, the addition of the synthesized powders in various concentrations to the culture media did not negatively impact the number of viable cells after 24 hours of incubation (compared with the control sample, in which the powder concentration was 0 μg/mL).

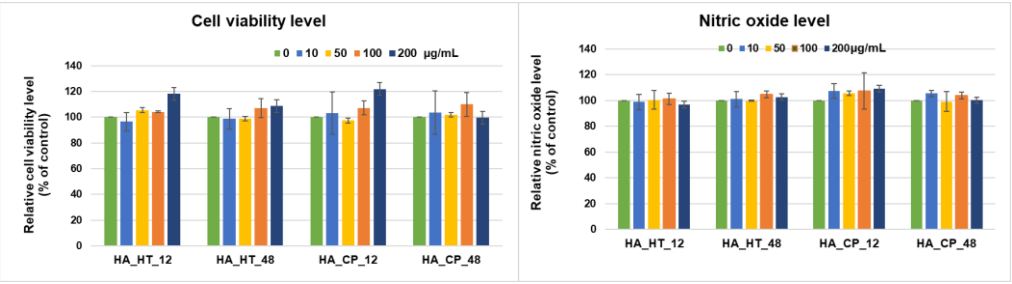

(a) (b)

Fig. 5. (a) Cell viability results obtained by MTT assay and (b) NO release measured by Griess assay after 24 hours of cell growth in the presence of 10, 50, 100, 200 μg/mL samples. Control sample 0 μg/mL(green). Results are presented as mean ± standard deviation of three independent experiments.

Moreover, the MC3T3-E1 osteoblasts proliferation increased when higher amounts of HA were added. Specifically, the samples aged for 12h showed the best results (cell viability reaching a maximum of 120%) at 200 μg/mL, while the

samples aged for 48h proved efficient at 100 μg/ mL. The amount of NO released in the culture media was assessed as a valuable indicator of inflammation and cell membrane damage after incubation with HA powders. Fig. 5b shows no significant changes in NO release after cell exposure to all samples, compared with the control sample (MC3T3-E1 osteoblasts without added powder), proving that the four specimens tested induce a low, almost physiological, inflammation effect.

Nevertheless, the observed compositional and morpho-structural similarities of the four tested specimens, stimulate a sameness in cellular viability and induce a less than 9% relative nitric oxide concentration, released as cytotoxic stress produced by powders over the viable cells culture.

4. Conclusions

This paper aimed to evaluate the effect of the aging method on synthetic hydroxyapatite properties. Specifically, two maturation methods, a classical one and an unconventional short time maturation at 135°C in microwave-assisted hydrothermal conditions were assessed. The results demonstrate the structural and compositional features of the obtained samples, which recommend them as prospective materials with medical applications as a bone substitute. The exposure to microwave irradiation determined a 100% increase in the crystallinity degree of the HA powders, with a crystallization tendency after [002] crystallographic direction. This aspect is also encountered in natural bone, along with an important content of carbonate groups, involved in both A and B type substitutions in HA lattice. The samples treated under microwave conditions also showed a higher level of relative cell viability and induced a lower inflammatory process than the control sample, which implies a better cytotoxic behavior compared to the classic matured samples. The synthesized HA nano-powders have proven their non-cytotoxicity and are prospective candidates as a bone substitute, either in their powder form or as a component of bio-composites.

Acknowledgment

This work is supported by the project ANTREPRENORDOC, in the framework of Human Resources Development Operational Program 2014-2020, financed from the European Social Fund under the contract number 36355/23.05.2019 HRD OP /380/6/13 – SMIS Code: 123847."

R E F E R E N C E S

[1] *A.H. Dewi, I.D. Ana*, „The use of hydroxyapatite bone substitute grafting for alveolar ridge preservation, sinus augmentation, and periodontal bone defect: A systematic review", Heliyon, 4 (2018) e00884.

[2] *S. Titsinides, G. Agrogiannis, T. Karatzas*, „Bone grafting materials in dentoalveolar reconstruction: A comprehensive review", Jpn Dent Sci Rev, 55 (2019) 26-32.

[3] *I.A. Neacsu, L.V. Arsenie, R. Trusca, I.L. Ardelean, N. Mihailescu, I.N. Mihailescu, C. Ristoscu, C. Bleotu, A. Ficai, E. Andronescu*, „Biomimetic Collagen/Zn(2+)-Substituted Calcium Phosphate Composite Coatings on Titanium Substrates as Prospective Bioactive Layer for Implants: A Comparative Study Spin Coating vs. MAPLE", Nanomaterials (Basel), 9 (2019).

[4*] J.G. Caton, G. Armitage, T. Berglundh, I.L.C. Chapple, S. Jepsen, K.S. Kornman, B.L. Mealey, P.N. Papapanou, M. Sanz, M.S. Tonetti*, „A new classification scheme for periodontal and peri-implant diseases and conditions - Introduction and key changes from the 1999 classification", J Clin Periodontol, 45 Suppl 20 (2018) S1-S8.

[5] *E.S. Bishop, S. Mostafa, M. Pakvasa, H.H. Luu, M.J. Lee, J.M. Wolf, G.A. Ameer, T.C. He, R.R. Reid*," 3-D bioprinting technologies in tissue engineering and regenerative medicine: Current and future trends", Genes Dis, 4 (2017) 185-195.

[6] *A. Pal, S. Paul, A.R. Choudhury, V.K. Balla, M. Das, A. Sinha*, „Synthesis of hydroxyapatite from Lates calcarifer fishbone for biomedical applications", Materials Letters, 203 (2017) 89-92.

[7] *A.I. Adeogun, A.E. Ofudje, M.A. Idowu, S.O. Kareem*, „Facile Development of Nano Size Calcium Hydroxyapatite Based Ceramic from Eggshells: Synthesis and Characterization, Waste and Biomass Valorization", 9 (2017) 1469-1473.

[8] *N. Kourkoumelis, X. Zhang, Z. Lin, J. Wang*, „Fourier Transform Infrared Spectroscopy of Bone Tissue: Bone Quality Assessment in Preclinical and Clinical Applications of Osteoporosis and Fragility Fracture", Clinical Reviews in Bone and Mineral Metabolism, 17 (2019) 24-39.

[9] *P. Moerbeck-Filho, S.C. Sartoretto, M.J. Uzeda, M. Barreto, A. Medrado, A. Alves, M.D. Calasans-Maia*, „Evaluation of the In Vivo Biocompatibility of Amorphous Calcium Phosphate-Containing Metals", J Funct Biomater, 11 (2020).

[10] *M. Mosina, J. Locs*, „Synthesis of Amorphous Calcium Phosphate: A Review", Key Engineering Materials, 850 (2020) 199-206.

[11] *G. Karunakaran, G.S. Kumar, E.-B. Cho, Y. Sunwoo, E. Kolesnikov, D. Kuznetsov*, „Microwave-assisted hydrothermal synthesis of mesoporous carbonated hydroxyapatite with tunable nanoscale characteristics for biomedical applications", Ceramics International, 45 (2019) 970-977.

[12] *K.W. Goh, Y.H. Wong, S. Ramesh, H. Chandran, S. Krishnasamy, S. Ramesh, A. Sidhu, W.D. Teng*, „Effect of pH on the properties of eggshell-derived hydroxyapatite bioceramic synthesized by wet chemical method assisted by microwave irradiation", Ceramics International, 47 (2021) 8879-8887.

[13] *C.R. Dumitrescu, I.A. Neacsu, V.A. Surdu, A.I. Nicoara, F. Iordache, R. Trusca, L.T. Ciocan, A. Ficai, E. Andronescu*, „Nano-Hydroxyapatite vs. Xenografts: Synthesis, Characterization, and In Vitro Behavior", Nanomaterials, 11(9) (2021), 2289.

[14] *T.J.U. Thompson, M. Gauthier, M. Islam*, „The application of a new method of Fourier Transform Infrared Spectroscopy to the analysis of burned bone", Journal of Archaeological Science, 36 (2009) 910-914.

[15] *A. Antonakos, E. Liarokapis, T. Leventouri*, „Micro-Raman and FTIR studies of synthetic and natural apatites", Biomaterials, 28 (2007) 3043-3054.

[16] *C. Suresh Kumar, K. Dhanaraj, R.M. Vimalathithan, P. Ilaiyaraja, G. Suresh*, „Hydroxyapatite for bone-related applications derived from seashell waste by simple precipitation method", Journal of Asian Ceramic Societies, 8 (2020) 416-429.

[17] *A.R. Noviyanti, N. Akbar, Y. Deawati, E.E. Ernawati, Y.T. Malik, R.P. Fauzia, Risdiana*, „A novel hydrothermal synthesis of nanohydroxyapatite from eggshell-calcium-oxide precursors", Heliyon, 6 (2020) e03655.
[18] *H.S. Sohn, J.K. Oh*, „Review of bone graft and bone substitutes with an emphasis on fracture surgeries", Biomater Res, 23 (2019) 9.
[19] *J.-K. Han, H.-Y. Song, F. Saito, B.-T. Lee*, „Synthesis of high purity nano-sized hydroxyapatite powder by microwave-hydrothermal method", Materials Chemistry and Physics, 99 (2006) 235-239.
[20] *M.A.M. Castro, T.O. Portela, G.S. Correa, M.M. Oliveira, J.H.G. Rangel, S.F. Rodrigues, J.M.R. Mercury*, „Synthesis of hydroxyapatite by hydrothermal and microwave irradiation methods from biogenic calcium source varying pH and synthesis time", Boletín de la Sociedad Española de Cerámica y Vidrio, (2020).
[21] *H.-P. Yu, Y.-J. Zhu, B.-Q. Lu*, „Highly efficient and environmentally friendly microwave-assisted hydrothermal rapid synthesis of ultralong hydroxyapatite nanowires", Ceramics International, 44 (2018) 12352-12356.
[22] *F. Cestari, F. Agostinacchio, A. Galotta, G. Chemello, A. Motta, V.M. Sglavo*, „Nano-Hydroxyapatite Derived from Biogenic and Bioinspired Calcium Carbonates: Synthesis and In Vitro Bioactivity", Nanomaterials (Basel), 11 (2021).
[23] *M.A.M. Castro, T.O. Portela, G.S. Correa, M.M. Oliveira, J.H.G. Rangel, S.F. Rodrigues, J.M.R. Mercury*, „Synthesis of hydroxyapatite by hydrothermal and microwave irradiation methods from biogenic calcium source varying pH and synthesis time", Boletín de la Sociedad Española de Cerámica y Vidrio, (2020).
[24] *F.E. Tabaght, K. Azzaoui, A. Elidrissi, O. Hamed, E. Mejdoubi, S. Jodeh, N. Akartasse, M. Lakrat, A. Lamhamdi*, „New nanostructure based on hydroxyapatite modified cellulose for bone substitute, synthesis, and characterization", International Journal of Polymeric Materials and Polymeric Biomaterials, (2020) 1-12.
[25] *N.K. Nga, N.T. Thuy Chau, P.H. Viet*, „Facile synthesis of hydroxyapatite nanoparticles mimicking biological apatite from eggshells for bone-tissue engineering", Colloids Surf B Biointerfaces, 172 (2018) 769-778.